Talanta 80 (2010) 2113–2119

Contents lists available at ScienceDirect

Talanta

journal homepage: www.elsevier.com/locate/talanta

Electrochemical biosensor based on nanogold-modified poly-eriochrome black T film for BCR/ABL fusion gene assay by using hairpin LNA probe

Liqing Lin[a], Jing Chen[a], Qihuang Lin[a], Wei Chen[a], Jinghua Chen[a], Hong Yao[a], Ailin Liu[a], Xinhua Lin[a,*], Yuanzhong Chen[b,**]

[a] Department of Pharmaceutical Analysis, Faculty of Pharmacy, Fujian Medical University, Fuzhou 350004, China
[b] Fujian Institute of Hematology, The Affiliated Union Hospital of Fujian Medical University, Fuzhou 350001, China

ARTICLE INFO

Article history:
Received 3 August 2009
Received in revised form 28 October 2009
Accepted 3 November 2009
Available online 13 November 2009

Keywords:
Electrochemical biosensor
NG/EBT film
BCR/ABL fusion gene
Locked nucleic acids

ABSTRACT

A novel electrochemical biosensor is described for detection of breakpoint cluster region gene and a cellular abl (BCR/ABL) fusion gene in chronic myelogenous leukemia (CML) by using thiolated-hairpin locked nucleic acids (LNA) as the capture probe. The hairpin LNA probe was immobilized on the nanogold (NG)/poly-eriochrome black T (EBT) film-modified glassy carbon electrode (GCE). The immobilized LNA probe could selectively hybridize with its target DNA on LNA/NG/EBT/GCE surface. The immobilization and hybridization of the LNA probe were characterized with cyclic voltammetry and electrochemical impedance spectroscopy. The hybridization of the immobilized LNA probe with the target DNA was detected by differential pulse voltammetry with the electroactive methylene blue as an indicator. The results indicated this new method has excellent specificity for single-base mismatch and complementary after hybridization, and a high sensitivity. This novel electrochemical biosensor has been used for assay of PCR real sample with satisfactory result.

1. Introduction

CML is a clonal myeloproliferative disorder, resulting from the neoplastic transformation of the primitive hemopoietic stem cell [1–3]. The chimeric oncogene breakpoint cluster region gene and a cellular abl gene (BCR/ABL) is the traditional gene existed in almost all cases of CML patients [4,5]. Thus, detection of BCR/ABL fusion gene will afford an early diagnosis and monitor of the disease. In recent years, there has been significant progress in developing nucleic acid hybridization biosensors for the rapid and accurate detections of specific gene sequence [6,7]. As with other types of biosensors, high selectivity is crucial for the success of hybridization biosensors [8]. The selectivity of nucleic acid hybridization assays depends primarily on the selection of the probe and then of the hybridization conditions. Thus, the design of the probe is the most important pre-analytical step. Recently, some reports described the synthesis and hybridization of a novel nucleotide termed LNA [9,10].

LNA is a nucleic acid analogue of RNA, in which the furanose ring of the ribose sugar is chemically locked by the introduction of a methylene linkage between 2′-oxygen and 4′-carbon. The covalent bridge effectively 'locks' the ribose in the N-type (3-endo) conformation that is dominant in A-form DNA and RNA. This conformation enhances base stacking and phosphate backbone pre-organization and results in improved affinity for complementary DNA or RNA sequences, with each LNA substitution increasing the melting temperatures (T_m) by as much as 3.0–9.6 °C [11,12]. LNA bases can be interspersed with DNA bases, allowing binding affinity to be tailored for individual applications. Due to the very high affinity of the LNA molecules, it demonstrates that LNA probes hybridize with very high affinity to perfectly complementary targets, and at the same time shows an extraordinary specificity to discriminate the targets that differ by a single-base.

Moreover, sensitive detection of specific gene sequence on the basis of the hybridization reaction is another key issue. Increasing the immobilization amount and controlling over the molecular orientation of probe oligonucleotides would improve the detection sensitivity [13,14]. In the DNA sequence detection, the nanogold not only can act as the immobilizing carrier to increase the immobilization amount of the DNA probe but also can serve as the signal particle to magnify the detection signal and lower the detection limit [15,16]. Therefore, in this article, we introduce a method of immobilizing the LNA probe with nanogold bound to the poly-EBT film on the GCE. Due to the rich electroactive center and three-dimensional available field potential, the polymerized film-modified electrode has stable performance with good infusible and insoluble capability. EBT has been used in the biological electro-

* Corresponding author. Tel.: +86 591 22862016; fax: +86 591 22862016.
** Corresponding author. Tel.: +86 591 83357896; fax: +86 591 83357896.
E-mail addresses: xinhua63@163.com (X. Lin), chenyz@pub3.fz.fj.cn (Y. Chen).

0039-9140/$ – see front matter © 2009 Published by Elsevier B.V.
doi:10.1016/j.talanta.2009.11.017

analysis [17]. Nanogold can integrate with the biological active components. LNA probe can form a powerful Au–S covalent bond with hydrosulfuryl and the excellent biocompatibility of nanogold with LNA. So a novel electrochemical DNA biosensor based on the NG/EBT/GCE was developed for recognition of target DNA by using hairpin LNA as the capture probe for hybridization with BCR/ABL fusion gene in CML.

2. Materials and methods

2.1. Reagents and apparatus

Methylene blue (MB) and $HAuCl_4{\cdot}4H_2O$ were purchased from Sigma (USA). Sodium dodecyl sulfate (SDS), sodium citrate and eriochrome black T (EBT) was purchased from Shanghai Chemical Reagents Company (China). The oligonucleotides were synthesized by Shanghai Shenggong Biotechnology Co. (Shanghai, China), and it has the following sequences:

Thiolated-hairpin LNA probe: 5′-SH-C**T**$^{\text{L}}$G**C**$^{\text{L}}$AG**A**$^{\text{L}}$GT**T**$^{\text{L}}$CA**A**$^{\text{L}}$AA **G**$^{\text{L}}$CC **C**$^{\text{L}}$TT CGC AG-3′, (L: 2′-*O*,4′-*C*-methylene·(D-ribofuranosyl) nucleotides LNA. LNA probe is a DNA–LNA chimera, but for brevity it will be called LNA probe [18]. Bold letters represent LNA bases. Underlined letters are bases for stem). Complementary target: 5′-GAA GGG CTT TTG AAC TCT-3′, single-base mismatch: 5′-GAA GGG ATT TTG AAC TCT-3′, non-complementary: 5′-ACG TAA TCC CCA GCT CTC-3′.

The oligonucleotide stock solutions (100 μM) were prepared with 20 mM Tris–HCl, 10 mM $MgCl_2$, pH 8.0 and kept frozen. Real samples were kindly donated by Fujian Institute of Hematology, the Affiliated Union Hospital of Fujian Medical University. Millipore Milli-Q water was used in all experiments. Unless otherwise indicated, all reagents and solvents were purchased in their highest available purity and used without further purification.

A CHI 660C electrochemical analyzer (CH Instrument, USA), which was in connection with a GCE (3 mm diameter) as the working electrode, a Ag/AgCl reference electrode and a platinum wire auxiliary electrode, was used for the electrochemical measurement.

2.2. The preparation of surface of biosensor and its immobilization with LNA probe

The scheme for preparation of the electrochemical DNA biosensor is illustrated in Fig. 1. The surface modification of the GCE was performed by procedure reported in Ref. [17]. Before surface modification, the GCE was polished in sequential order with 1.0, 0.3 and 0.05 μm alumina (AlfaAesar, USA). The electrode was thoroughly washed with water, sonicated in ethanol, and finally dried thoroughly under N_2 flow. Then, GCE was polarized in 0.1 M H_2SO_4 by cyclic scanning between −0.40 and +1.50 V for 25 cycles and scanned in 0.1 M NaOH under the same conditions for 25 times to obtain the pretreated electrode. The poly-EBT was electropolymerized onto pretreated GCE in the presence of 0.1 M NaOH containing 0.5 mM EBT on the same conditions. The obtained electrode was donated as EBT/GCE. The EBT/GCE was immersed into 1% NG solution prepared by the citrate reduction of $HAuCl_4$ for 4 h [19,20]. NG was electro-deposited on the surface of EBT/GCE for 100 s at 0.15 V to prepare NG/EBT/GCE. Apparently a mount of nanogold provides an easier way to immobilize the probe LNA with thiol groups at the 5′ end [21].

Immobilization of the LNA probe on the NG/EBT/GCE surface is described as follows. 10 μl of 1.0 μM probe LNA was dropped on the surface of NG/EBT/GCE and air-dried to dryness. Then the electrode was washed with 0.1% SDS solution for 5 min to wash out the unimmobilized LNA probe. The probe modified electrode was donated as LNA/NG/EBT/GCE.

Table 1
Melting temperatures of the LNA and DNA capture probe against complementary and single-base-mismatched DNA targets.

Probe type	T_m (°C)		ΔT_m (°C)
	Complementary target	Single-base mismatch	
DNA	50.3	44.7	5.6
LNA	78.8	38.1	40.7

The hybridization was performed by pipetting 10 μl of different concentrations of complementary target (cDNA) onto the LNA/NG/EBT/GCE for 1 h at 60 °C. Thus, a double-stranded LNA-cDNA (dsDNA)/NG/EBT/GCE was obtained. The electrode surface was then washed with 0.1% SDS for 5 min to remove the unbound oligonucleotides. The same protocol as above-mentioned was applied to LNA/NG/EBT/GCE for hybridization with one-base mismatch and also with non-complementary sequences.

2.3. MB accumulation and voltammetric transduction

MB for DNA hybridization detection is illustrated in Fig. 1. MB was accumulated onto the surface of hybrid-modified NG/EBT/GCE by immersing the electrode into stirred 20 mM Tris–HCl (pH 7.0) containing 20.0 μM MB with 50 mM NaCl for 5 min without applying any potential. In the optimal condition, the concentration of MB was chosen as 20.0 μM and the accumulation time of MB was chosen as 5 min for optimum analytical performance. After accumulation of MB, the electrode was rinsed with 0.1 M PBS to remove the non-specific MB and subjected to electrochemical measurement.

3. Results and discussion

3.1. Spectrophotometric characterization of DNA and LNA probes

Melting temperature (T_m) is the temperature at which double-stranded DNA is changed (50%) to single-stranded DNA. The denaturation of double-stranded DNA can be conveniently monitored by the sharp increase in absorbance at 260 nm (the absorbance maximum for DNA) using the spectrophotometer UV–Vis Varian Cary 100 (Varian). T_m for the hybridization of LNA with their complemental DNA were examined to confirm their potential for selective recognition of complementary sequences. From Fig. 2 and Table 1, the T_m value of the LNA probe (78.8 °C) was greatly higher than that of its corresponding DNA probe (50.3 °C). Comparing with the analogous DNA–DNA hybrids, T_m value for LNA binding to DNA was increased 28.5 °C, which was equivalent to 4.1 °C per LNA compared to DNA duplexes [22,23]. T_m value for LNA binding to single-base mismatch was decreased to 38.1 °C. Therefore, the affinity and specificity of the LNA probes can be confirmed by measurement of duplex T_m.

Theoretically, the optimum hybridization temperature was about 20 °C lower than T_m. The T_m value of the LNA probe binding to complementary target was 78.8 °C, while for single-base mismatch was decreased to 38.1 °C, Therefore, the theoretical hybridization temperature was 58.8 and 18.1 °C for the complementary target and single-base mismatch, respectively. Accordingly, 60 °C was selected as hybridization temperature [10]. At this temperature, hybridization could be occurred only for the complementary target strand but not for the single-base mismatch. Therefore, the hybridization specificity was dramatically increased.

3.2. Covalent modification of GCE with EBT

The covalent modification of the GCE was performed by repeated cyclic voltammograms scanning over the range of −0.4

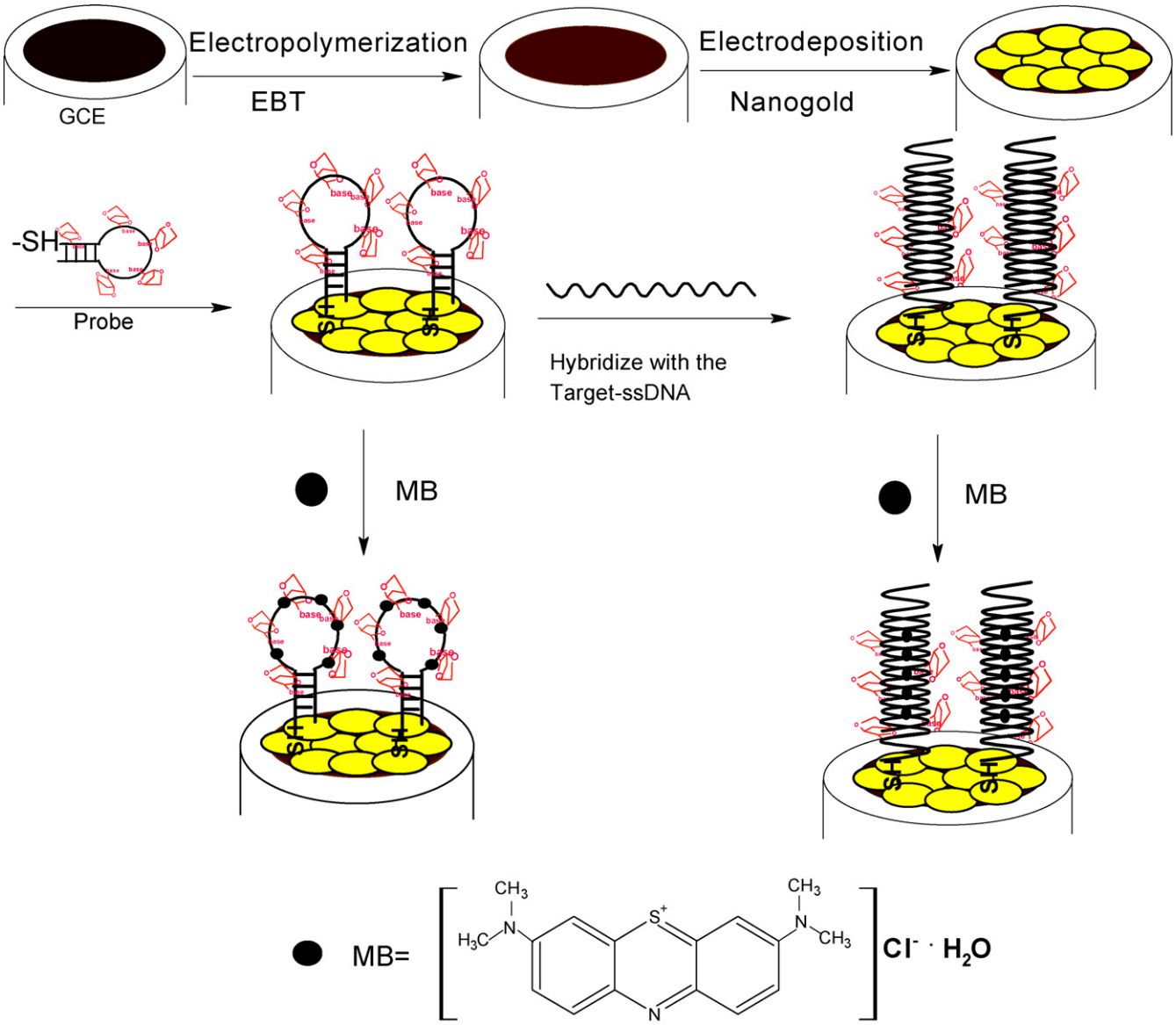

Fig. 1. Scheme of the procedure for the fabrication of DNA biosensor.

to 1.5 V at 100 mV/s for 25 cycles in 0.1 M NaOH containing 0.5 mM EBT. Typically, it was found that when cyclic time was increased, the peak currents gradually decreased. This phenomenon implies the formation of poly-EBT membrane on GCE [17]. The electrodeposited behavior of EBT at the GCE was similar to some reports referring to the electrochemical responses of a few azo compounds at solid electrode [24]. The reaction mechanism could be explained as follows: (1) EBT was first deposited at the surface of GCE and oxidized to form a benzoquinone diimine structure; (2) and then the benzoquinone diimine structure was reduced to EBT at the surface of GCE. The peak currents trended to be stable after 20 scans, which indicated that the GCE surface has been modified with a sulfonic-terminated monolayer to form the EBT/GCE.

3.3. *Electrochemical characterization of different modified electrodes*

Cyclic voltammograms (CV) of 10 mM $[Fe(CN)_6]^{3-/4-}$ redox couple in 0.1 M phosphate buffer solution at a bare GCE (a), EBT/GCE (b), NG/EBT/GCE (c), LNA/NG/EBT/GCE (d) and dsDNA/NG/EBT/GCE (e) were shown in Fig. 3A. Curve a shows that a symmetric, reversible

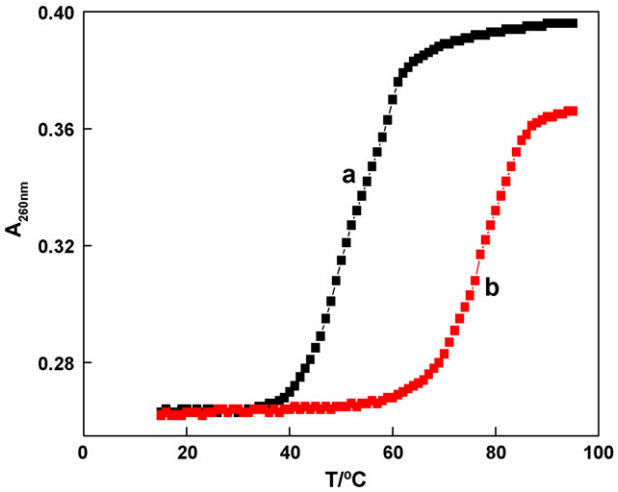

Fig. 2. Melting curves of DNA–DNA (a), LNA–DNA duplex (b).

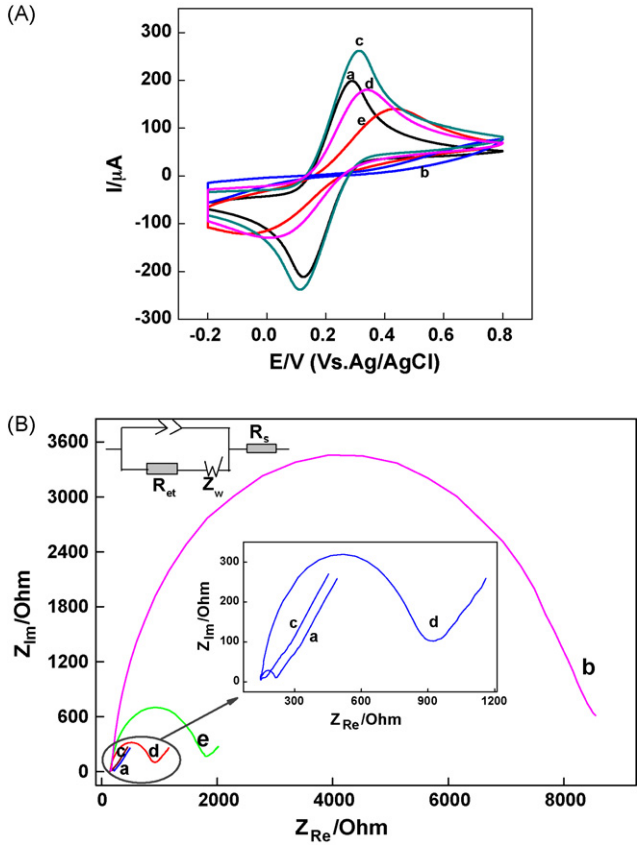

Fig. 3. (A) CV of 10 mM $[Fe(CN)6]^{3-/4-}$ for bare GCE (a), EBT/GCE(b), NG/EBT/GCE (c), LNA/NG/EBT/GCE (d) and dsDNA/NG/EBT/GCE (e). (B) Impedance plots on bare GCE (a), EBT/GCE (b), NG/EBT/GCE (c), LNA/NG/EBT/GCE (d) and dsDNA/NG/EBT/GCE (e) in 10 mM $[Fe(CN)6]^{3-/4-}$.

voltammogram was obtained for a bare GCE. Curve b clearly shows that the electron transfer of $[Fe(CN)_6]^{3-/4-}$ is completely blocked on the EBT/GCE. It can be explained by the electrostatic interactions between the modified surface and $[Fe(CN)_6]^{3-/4-}$. As it known, the pK_a value of R–SO_3H (R: alkyl or aryl groups) is usually between 3 and 4. When the solution pH was equal to 7, the –SO_3Na group of poly-(EBT) film could dissociate favorably into a negative charge group –SO_3^-. Thus, on the negatively charged EBT film, the electrostatic repulsion resists access of $[Fe(CN)_6]^{3-/4-}$ to the electrode surface and blocks its electron-transfer on the electrode surface. Curve c is the CV curve of the NG/EBT/GCE electrode in the same solution as above. The CV peak of curve c was much higher than that of curve b. This implies that NG had been successfully modified onto EBT film, resulting in the electrode having a larger electroactive surface and higher conductivity. When the LNA probe immobilized on the NG/EBT/GCE, compared with bare GCE and NG/EBT/GCE, the peak current decreased and the potential deviation increased (curve d). That is, the LNA probe had negative charge, so hampered $[Fe(CN)_6]^{3-/4-}$ to participate the electrode reaction. These results suggest that the NG/EBT/GCE surface is well covered with the LNA probe. After hybridization, there were more negative charges on the surface and the dsDNA modified layer became thicker. These two factors provide an effective barrier to electron-transfer of $[Fe(CN)_6]^{3-/4-}$ in solution (curve e).

Electrochemical impedance spectroscopy (EIS) can give information on the impedance changes of the electrode surface in the modification process. So EIS was also used to evaluate the interfacial electron-transfer efficiency at different stages of biosensor preparation [25]. Fig. 3B shows the typical EIS results of the bare GCE (a), EBT/GCE (b), NG/EBT/GCE (c), LNA/NG/EBT/GCE (d) and dsDNA/NG/EBT/GCE (e), respectively, which were obtained in a solution of 10 mM $[Fe(CN)_6]^{3-/4-}$ at a potential of 0.22 V (versus Ag/AgCl) in the frequency range of 0.1–10^5 Hz. The electron-transfer resistance (R_{et}) of the bare GCE was estimated to be 63 Ω (curve a). When a bare GCE was electropolymerized with EBT for 25 cyclic times, the electron transfer resistance increased significantly (R_{et} = 8386 Ω). The surface coverage (θ) of EBT film on a bare GCE can be calculated from the EIS in terms of the equation [26]

$$\theta = \frac{1 - R_{et}^{Bare}}{1 - R_{et}^{EBT}} \quad (1)$$

Using Eq. (1), the coverage was calculated to be 99.28%. When the gold nanoparticles was assembled on the EBT/GCE, the R_{et} value was found to be 16 Ω (curve c). As compared with curve a, the R_{et} value of the curve c reduced obviously. This might be due to the presence of nanoparticles playing an important role in accelerating the transfer of the electrons, thus decreasing the resistance of the NG/EBT/GCE to $[Fe(CN)_6]^{3-/4-}$. After the LNA probes were immobilized on the NG/EBT/GCE, its R_{et} value was 758 Ω (curve d), which was much larger than that of the curve c. The negatively charged phosphate backbone of the LNA probe prevented $[Fe(CN)_6]^{3-/4-}$ from reaching the electrode surface during the redox process, and therefore led to the obvious increase of R_{et} value. After hybridization, there were more negative charges on the surface and the DNA modified layer became thicker. These led to the further increase of R_{et} value. These results are in agreement with the CV data.

3.4. Hairpin LNA probe versus hairpin DNA probe

To clarify the role of the DNA sequence with locked nucleic acids modified probe (LNA probe), we tested the same sensing scheme immobilizing a DNA sequence that has no locked nucleic acids as probe (DNA probe) on the surface of NG/EBT/GCE. The experiment was performed with single-base mismatch sequences to investigate whether or not LNA probe improves the selectivity of the assay. Using DNA probe, the voltammetric signal obtained for single-base mismatch was found to be only about 1.42 times higher than the signal obtained for the same concentration of complementary target (see Fig. 4A). At the same time, the signal for the single-base mismatch was significantly increased when LNA was used as probe (see Fig. 4B). These data clearly show the high selectivity of LNA probe for the complementary target and single-base mismatch sequences compared with DNA probe. So in this study, we study the hybridization specificity by using LNA as the capture probe for detection of BCR/ABL fusion gene. The enhanced selectivity can be attributed to the LNA, LNA monomer contains a methylene bridge that connects the 2′-oxygen with the 4′-carbon of the ribose ring of RNA. This bridge results in a locked 3′-endo conformation, reducing the conformational flexibility of the ribose and increasing the degree of local organization of the phosphate backbone [27]. This entropic constraint leads to improving the binding to complementary RNA and DNA sequences.

3.5. The CV study of MB interacted with the LNA/NG/EBT/GCE along with change of scan rate

It had been reported that MB interacted in a different way with ssDNA and dsDNA [15,28]. So MB was used as an electrochemical indicator to study hybridization between LNA and target DNA. LNA modified NG/EBT/GCE electrode immersed in pH 7.0 Tris–HCl containing 20.0 μM MB and CV were collected with the scan rate of 50, 100, 200, 300, 400, 500, 600, 700 and 800 mV s^{-1}. As shown in Fig. 5A, a pair of evident oxidoreduction peak appeared, and the peak current increased along with the increasing of the scan rate. The plot of cathodic peak current (I) versus scan rate (v) is linear

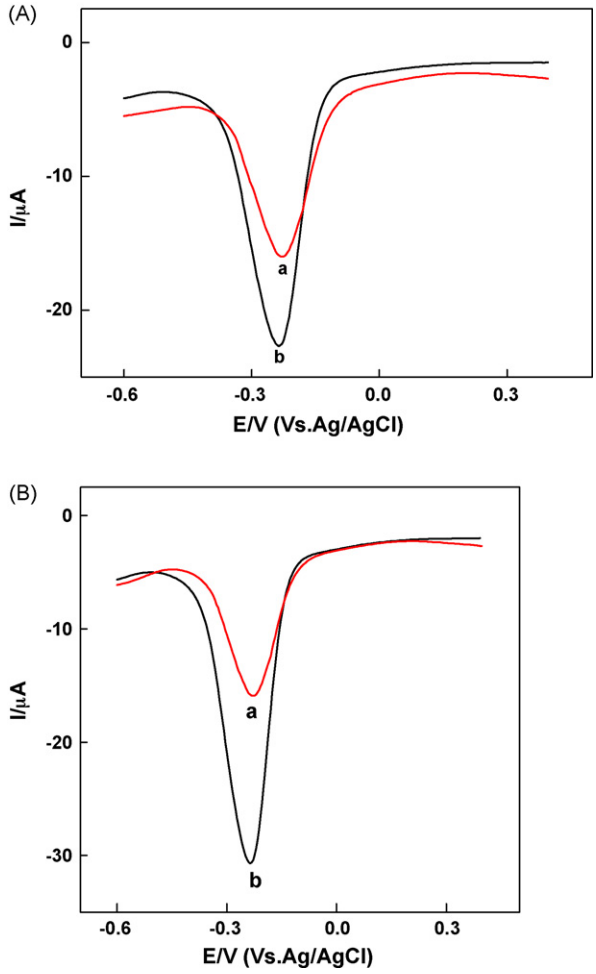

Fig. 4. (A) DPV of 20 μM MB at a DNA/NG/EBT/GCE hybridization with the complementary target (a) and single-base mismatch (b). (B) DPV of 20 μM MB at a LNA/NG/EBT/GCE hybridization with the complementary target (a) and single-base mismatch (b).

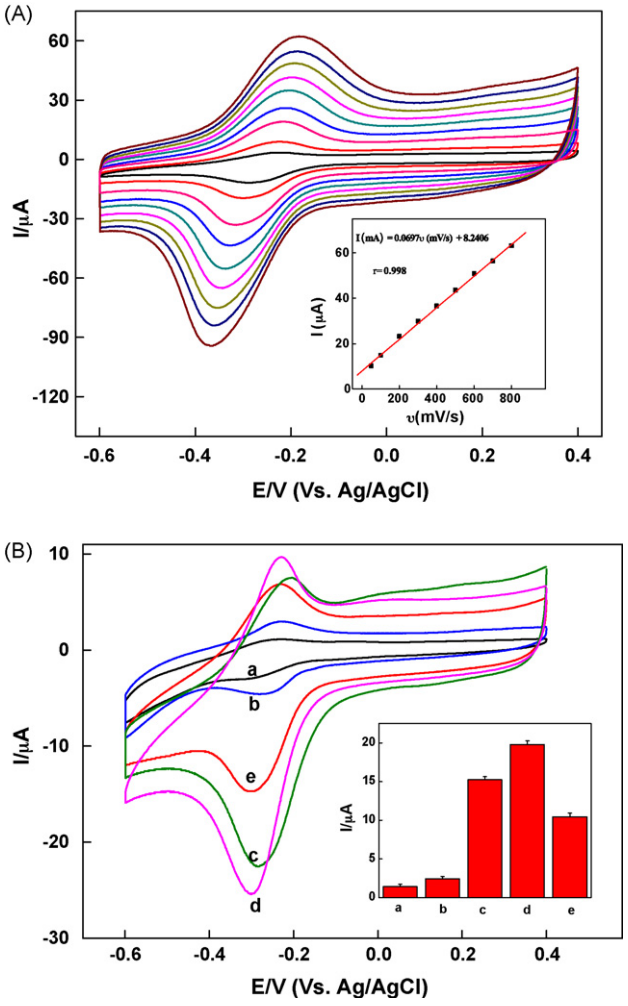

Fig. 5. (A) CV of 20 μM MB in 20 mM Tris–HCl buffer (pH 7.0) at the LNA probe modified NG/EBT/GCE surface with increasing scan rate from inner to outer: 50, 100, 200, 300, 400, 500, 600, 700, 800 mV s^{-1}. Inset shows plot of reduction peak current versus scan rate. (B) CV of 20 μM MB at the bare GCE (a), EBT/GCE (b), NG/EBT/GCE (c), LNA/NG/EBT/GCE (d) and dsDNA/NG/EBT/GCE (e). scan rate: 100 mV s^{-1}. Insert: corresponding histograms of the reduction peak currents.

(see Fig. 5A inset), indicating that MB was strongly bound to the LNA modified NG/EBT/GCE surface. Because MB could bind specifically to the LNA probe guanine bases [10,15]. The LNA probe was immobilized on the NG/EBT/GCE. So MB was strongly bound to the LNA modified NG/EBT/GCE surface.

3.6. Electrochemical behavior of MB on different electrodes

Fig. 5B shows the CV signals at different electrodes in 20 mM pH 7.0 Tris–HCl buffer solution containing 20.0 μM MB. It can be seen that a pair of weak redox peaks of MB was observed at the bare GCE (curve a) and EBT/GCE (curve b). For NG/EBT/GCE (curve c), the redox peak currents of MB were greatly enhanced. In addition, the immobilization of LNA probe on the NG/EBT/GCE modified electrode surface resulted in an increase in the peak currents of MB (curve d). It was attributed to nanogold thin film could provide a well platform for LNA probe immobilization and the electrostatic interaction between the negatively charged phosphate backbone of LNA and MB cation. At the same time, many more free guanine bases of LNA molecules were exposed out and had a strong affinity with MB, hence the greatest amount of MB accumulation occurs at this surface [29]. Therefore, the highest MB oxidoreduction signal was observed with LNA probe on NG/EBT/GCE. However, a significant decrease in the voltammetric peak current of MB was observed after complementary target sequence was allowed to hybridize with the LNA/NG/EBT/GCE (curve e). The decrease of current signal after hybridization was due to the inaccessibility of the guanine bases in dsDNA. This decrease is attributed to the steric inhibition of the reducible groups of MB packed between the bulky double helix of the hybrid. MB could bind specifically to the guanine bases and readily intercalate into dsDNA as well. Different binding modes of MB with LNA modified ssDNA and dsDNA resulted in variation in electrochemical responses.

3.7. Hybridization specificity of hairpin LNA probe

Hairpin LNA has high hybridization specificity because of its LNA and loop-stem structure [30], which can easily discriminate complementary oligonucleotide from single-base mismatch oligonucleotide. The selectivity of this assay was investigated by using the hairpin LNA as the capture probe to hybridize with various DNA sequences related to BCR/ABL fusion gene. Fig. 6A shows the differential pulse voltammetry (DPV) signal of MB at LNA/NG/EBT/GCE (d) and after hybridization with complementary target (a), single-base mismatch (b) and non-complementary (c). It is clear that curve d shows the highest peak current of MB on the LNA/NG/EBT/GCE, and after hybridization with complementary oligonucleotide, the peak current of MB is dramatically

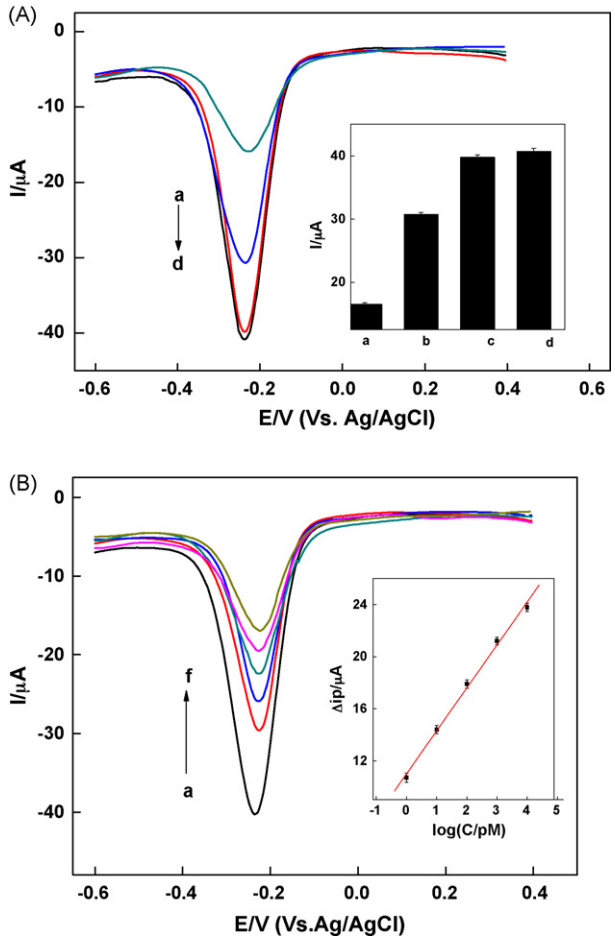

Fig. 6. (A) DPV of 20 μM MB at LNA/NG/EBT/GCE (d) and after hybridization with the complementary target (a), single-base mismatch (b) and non-complementary (c). Inset shows the bar graph of the peak current of MB when the LNA probe hybridized with different gene fragments. Error bars = ±relative standard deviation. (B) DPV of MB accumulated on the LNA after its hybridization with different concentration of the target sequence. Target concentration (*M*): (a) probe; (b) 1.0×10^{-12}; (c) 1.0×10^{-11}; (d) 1.0×10^{-10}; (e) 1.0×10^{-9}; (f) 1.0×10^{-8}. Inset shows the plot of the peak current of MB as a function of the target concentration. Error bars = ±relative standard deviation.

decreased (curve a). It can also easily discriminate the complementary oligonucleotide from single-base mismatch oligonucleotide. In the presence of oligonucleotide containing a single-base mismatch, significantly increased voltammetric signal can be observed (curve b), which indicates that the complete hybridization is not accomplished due to the base mismatch. So the hairpin LNA has high hybridization specificity for the complementary oligonucleotide and single-base mismatch oligonucleotide. In addition, as expected, no significant difference of peak current can be observed for the hairpin LNA probe and its hybridization with non-complementary (curve c), since no successful hybridization occurs due to the sequence mismatch between the hairpin LNA probe and non-complementary.

The sensitivity of this electrochemical biosensor for the target DNA was investigated by varying the target oligonucleotide concentration according to the procedure described in Section 2. The different current value obtained in the DPV response of MB after hybridization of LNA probe with target was recorded with three repetitive measurements. The current response decreased in proportion to the amount of the target sequence. The average current response shows excellent correlation with the amount of the complementary oligonucleotides in the range of 1.0×10^{-12}–1.0×10^{-8} M (Fig. 6B). The regression equation is

$$\Delta ip(\mu A) = 3.30(\log C/pM) + 11.0 \quad R = 0.9983$$

A detection limit of 1.0×10^{-13} M for the target DNA can be estimated using 3σ (where σ is the standard deviation of the blank solution, $n = 7$). The reproducibility of the biosensor for detection of 1.0×10^{-11} M target DNA is 7.35% ($n = 7$).

3.8. Detection of PCR products

This novel electrochemical biosensor based on the LNA probe on the NG/EBT/GCE has been used for assay of PCR product of real sample. When the hairpin LNA probe for BCR/ABL was immobilized and hybridized with real PCR samples in the hybridization step. The DPV signals of MB obtained from the LNA probe modified NG/EBT/GCE gave a mean average of 40.8 μA with a RSD of 5.12%. The DPV signals of MB obtained from the hybridization of the LNA probe with the positive and negative real samples gave mean average of 16.5 μA with RSD of 6.72% and 40.1 μA with RSD of 7.34%, respectively. The signal of MB for the LNA probe modified NG/EBT/GCE was much higher than that of LNA probe modified NG/EBT/GCE after hybridization with positive real sample. The decrease of DPV signals with positive real samples showed that the hybridization at the NG/EBT/GCE surface occurred and MB could not interact with the bound guanine base of the hybrid. The decrease in the reduction signal of MB was attributed to the steric inhibition of the reducible groups of MB because of the formation of hybrid at the NG/EBT/GCE surface. If the blood sample was negative, the negative real sample would not contain a target sequence complementary to the specific LNA probe. The hybridization between these negative real samples and the immobilized probe would not occur, so the signal of MB was higher than that of the positive real samples.

A gel electrophoresis method was performed. Fig. 7 shows the result of electrophoresis of PCR products. The PCR amplification products from a positive real sample (lane 3) show the light brands about 300 bp in the 1.5% agarose gel; however, the PCR amplification products from negative real sample (lane 2) do not present any brands in the gel. Thus, we can extrapolate that the primers have amplified specific band to discriminate the positive real sample

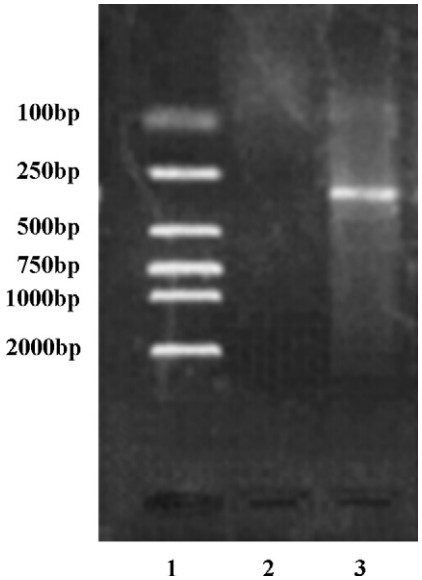

Fig. 7. Electrophoretogram of PCR amplified products. The lanes from left to right: lane 1: DL2000 DNA marker (the brands from up to down: 100 bp, 250 bp 500 bp, 750 bp, 1000 bp and 2000 bp); lane 2: negative real sample; lane 3: positive real sample.

from the negative real sample well. The results obtained from the gel electrophoresis are in good agreement with the ones obtained from the electrochemical DNA biosensor.

4. Conclusion

A novel electrochemical biosensor for detection of BCR/ABL fusion gene using hairpin LNA based on NG/EBT/GCE was fabricated. The hairpin LNA capture probe could selectively hybridize with its target DNA to form double-stranded DNA on NG/EBT/GCE surface. Since the quantities of LNA probe immobilized on the electrode surface can be greatly improved by nanogold-modified poly-EBT film approach. This novel DNA biosensor has higher sensitivity and better hybridization efficiency. The LNA probe was shown to be an effective biosensor for the detection of hybridization by using MB as the electrochemical indicator. This new method demonstrates its excellent specificity for single base mismatch and complementary after hybridization, and this method has been used for assay of PCR real sample with satisfactory result. The proposed method provided a simple, rapid tool for detection of DNA species in CML. It might have a promising future for investigation of DNA hybridization and solve the actual problem of the early diagnosis and prognosis monitor of CML and other diseases.

Acknowledgements

The authors gratefully acknowledge the financial support of the National Natural Science Foundation of China (20675015 and 20805006), the financial support of the National High Technology and Development of China (863 Project: 2006AA02Z4Z1 and 2008AA02Z433) and the Important Science and technology Foundation of Fujian Province (2008Y0045).

References

[1] P.J. Fialkow, S.M. Gartler, A. Yoshida, Proc. Natl. Acad. Sci. 58 (1967) 1468–1471.
[2] R.E. Champlin, D.W. Golde, Blood 65 (1985) 1039–1047.
[3] H.M. Kantarjian, A. Deisseroth, R. Kurzrock, Blood 82 (1993) 691–703.
[4] A. Butturini, B. Ralph, Leukemia Res. 20 (1996) 523–529.
[5] E.C. Jorge, T. Moshe, K. Hagop, Am. J. Med. 100 (1996) 555–570.
[6] Y. Zhang, N.F. Hu, Electrochem. Commun. 9 (2007) 35–41.
[7] H.L. Qi, X.X. Li, P. Chen, C.X. Zhang, Talanta 72 (2007) 1030–1035.
[8] J. Wang, Biosens. Bioelectron. 13 (1998) 757–762.
[9] S. Obika, D. Nanbu, Y. Hari, J. Andoh, K. Morio, T. Doi, T. Imanishi, Tetrahedron Lett. 39 (1998) 5401–5404.
[10] J.H. Chen, J. Zhang, K. Wang, X.H. Lin, L.Y. Huang, G.N. Chen, Anal. Chem. 80 (2008) 8028–8034.
[11] C.Y. James Yang, L. Wang, Y.R. Wu, Y.M. Kin, C.D. Medley, H. Lin, W.H. Tan, Nucleic Acids Res. 35 (2007) 4030–4041.
[12] J. Wengel, Acc. Chem. Res. 32 (1999) 301–310.
[13] R. Levicky, T.M. Herne, M.J. Tarlov, S.K. Satija, J. Am. Chem. Soc. 120 (1998) 9787–9792.
[14] T.A. Taton, C.A. Mirkin, R.L. Letsinger, Science 289 (2000) 1757–1760.
[15] N. Zhou, T. Yang, C. Jiang, M. Du, K. Jiao, Talanta 77 (2009) 1021–1026.
[16] H. Peng, L.J. Zhang, C. Soeller, J. Travas-Sejdic, Biomaterials 30 (2009) 2132–2148.
[17] H. Yao, Y.Y. Sun, X.H. Lin, Y.H. Tang, L.Y. Huang, Electrochim. Acta 52 (2007) 6165–6171.
[18] S. Fang, H.G. Lee, A.W. Wark, R.M. Corn, J. Am. Chem. Soc. 128 (2006) 14044–14046.
[19] J.J. Storhoff, R. Elghanian, R.C. Mucic, C.A. Mirkin, R.L. Letsinger, J. Am. Chem. Soc. 120 (1998) 1959–1964.
[20] M.H. Yang, J.H. Jiang, Y.S. Lu, Y. He, G.L. Shen, R.Q. Yu, Biomaterials 28 (2007) 3408–3417.
[21] B. Fang, S.F. Jiao, M.G. Li, Y. Qu, X.M. Jiang, Biosens. Bioelectron. 23 (2008) 1175–1179.
[22] Y. You, B.G. Moreira, M.A. Behlke, R. Owczarzy, Nucleic Acids Res. 34 (2006) e60.
[23] O. Richard, Biophys. Chem. 117 (2005) 207–215.
[24] A. Eriksson, L. Nyholm, Electrochim. Acta 44 (1999) 4029–4040.
[25] Z.S. Wu, F. Zheng, G.L. Shen, R.Q. Yu, Biomaterials 30 (2009) 2950–2955.
[26] C. Henke, C. Steinem, A. Janshoff, G. Steffan, H. Luftmann, M. Sieber, H.J. Galla, Anal. Chem. 68 (1996) 3158–3165.
[27] H. Kaur, A. Arora, J. Wengel, S. Maiti, Biochemistry 45 (2006) 7347–7355.
[28] F. Yan, A. Erdem, B. Meric, K. Kerman, M. Ozsoz, O.A. Sadik, Electrochem. Commun. 3 (2001) 224–227.
[29] N. Wei, J.H. Chen, J. Zhang, K. Wang, X.W. Xu, J.H. Lin, G.W. Li, X.H. Lin, Y.Z. Chen, Talanta 78 (2009) 1227–1234.
[30] R. Miranda-Castro, P. de-los-Santos-Alvarez, M.J. Lobo-Castanon, A.J. Miranda-Ordieres, P. Tunon-Blanco, Anal. Chem. 79 (2007) 4050–4055.